Supporting Information for

Computational differentiation of affinity and efficacy: Modelling PAM_16A activation of TMEM16A

Tanadet Pipatpolkai

Division of Physics and Applied Physics, School of Physical and Mathematical Sciences, Nanyang Technological University, Singapore

Email: tanadet.pipatpolkai@ntu.edu.sg

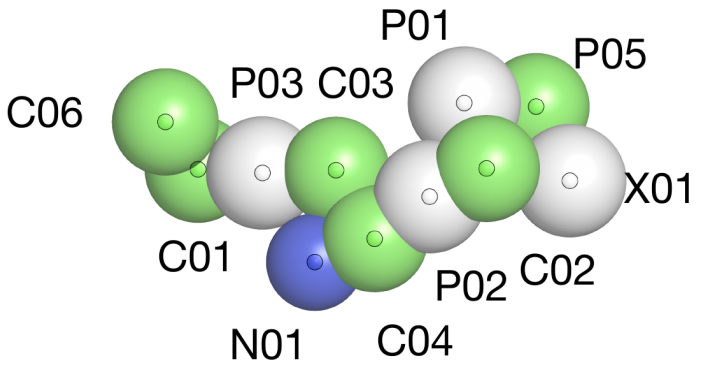

Supplementary Figure 1. MARTINI-3 coarse-grained representation of PAM_16A. The all-atom structure of PAM_16A mapped onto eleven coarse-grained beads using AutoMartini3. Beads are coloured by MARTINI bead type and labelled with the bead identifiers (P01–P03, C01–C06, N01, X01) that correspond to the [atoms] directive of Table S2, which lists the atom-to-bead assignments and the complete bonded topology.

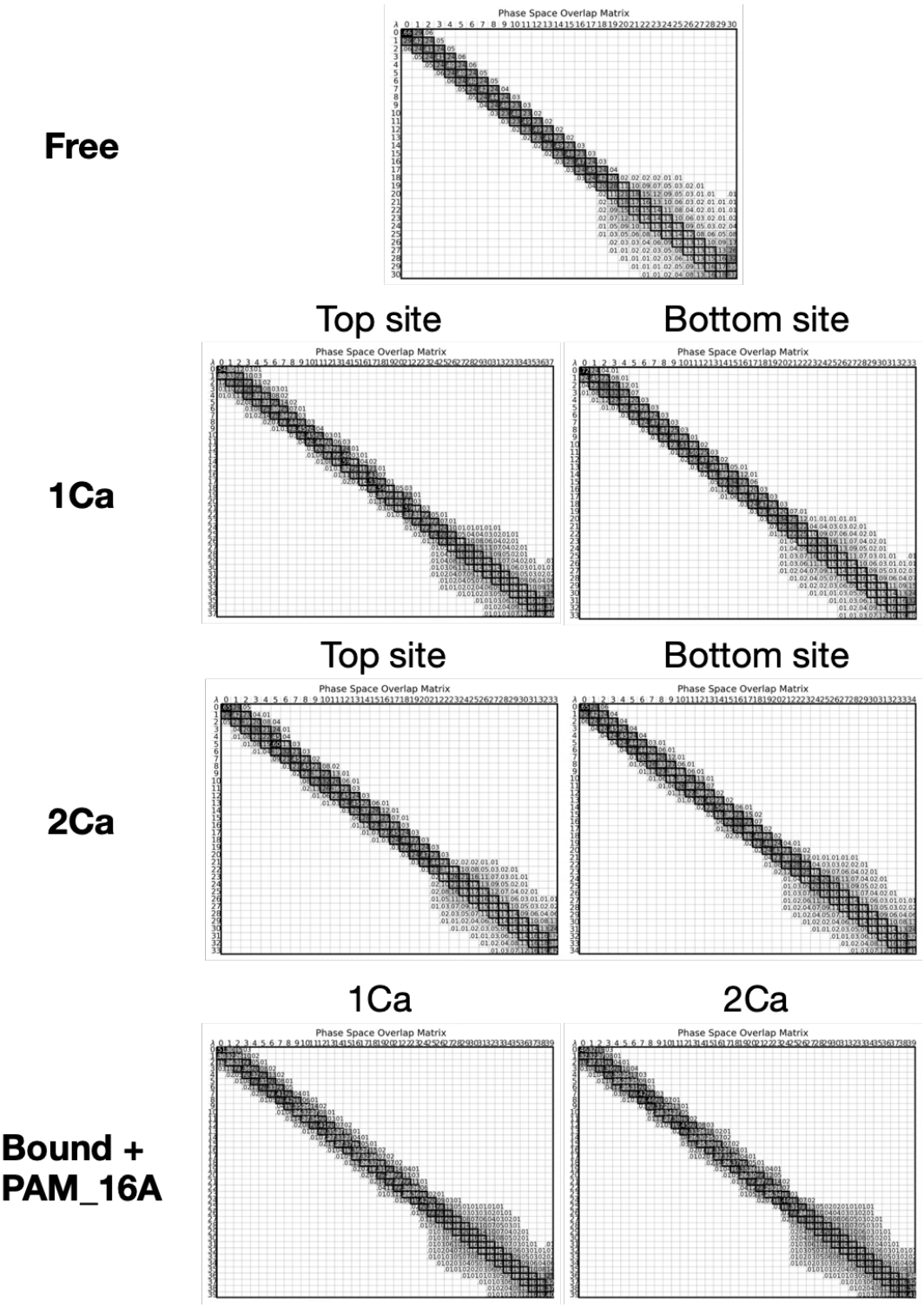

Supplementary Figure 2. Phase-space overlap matrix between neighbouring λ windows from the MBAR analysis; near-diagonal density confirms sufficient overlap for reliable estimates. Data shown are representative of n = 3 independent replicates.

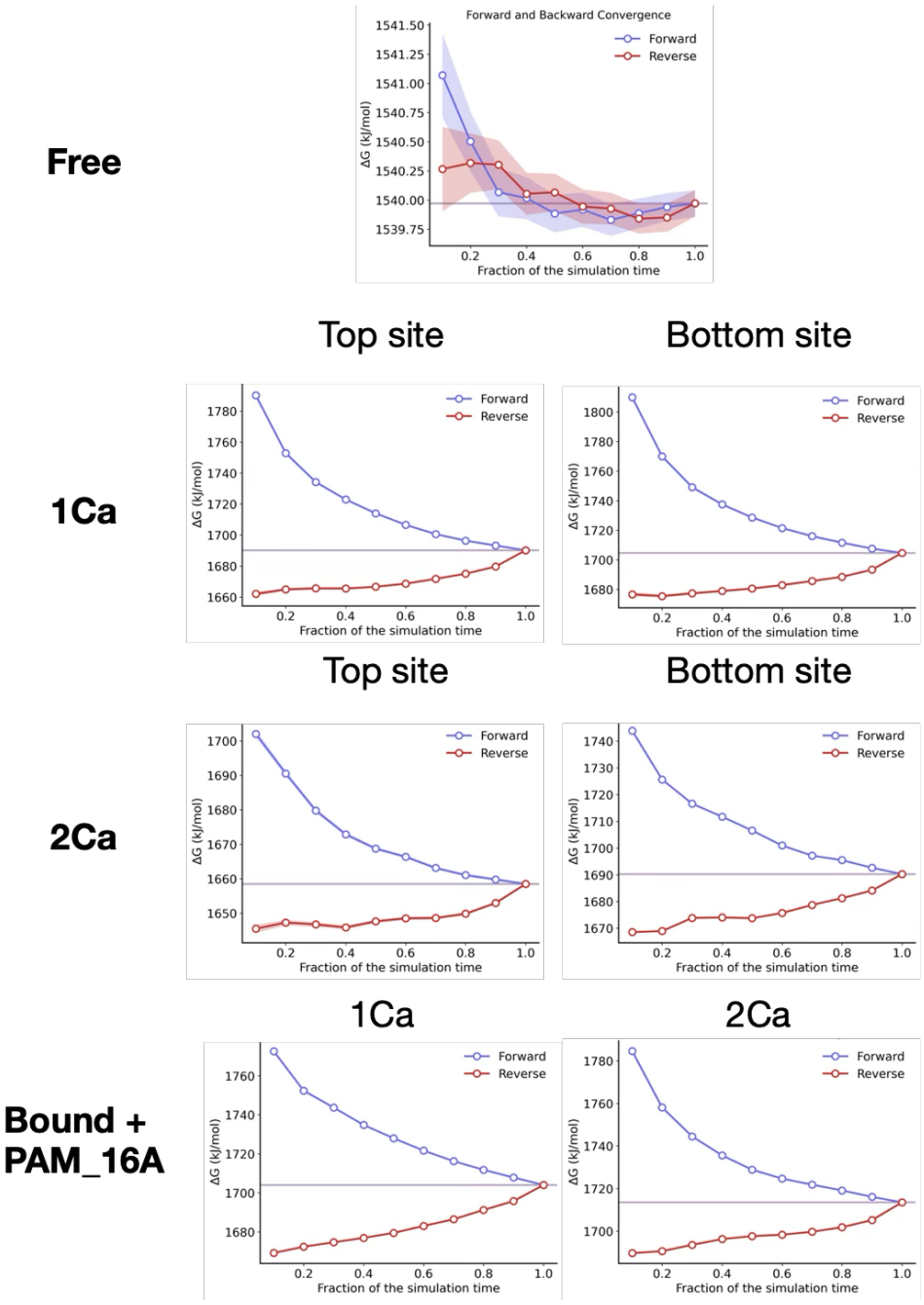

Supplementary Figure 3. Forward and reverse convergence of the calcium free energy perturbation (FEP) calculations. For each transformation, the free energy estimate (ΔG, MBAR) is plotted against the fraction of simulation time analysed from the start of the trajectories (Forward, blue) and from the end (Reverse, red); shaded bands denote the standard deviation and the horizontal line marks the estimate. Panels show the decoupling of Ca^{2+} in bulk water (Free) and in the channel without drug (Bound + Apo) and with PAM_16A (Bound + PAM_16A), for one or two bound calcium ions (1Ca, 2Ca) perturbed at the top or bottom site; one representative replicate is shown per condition.

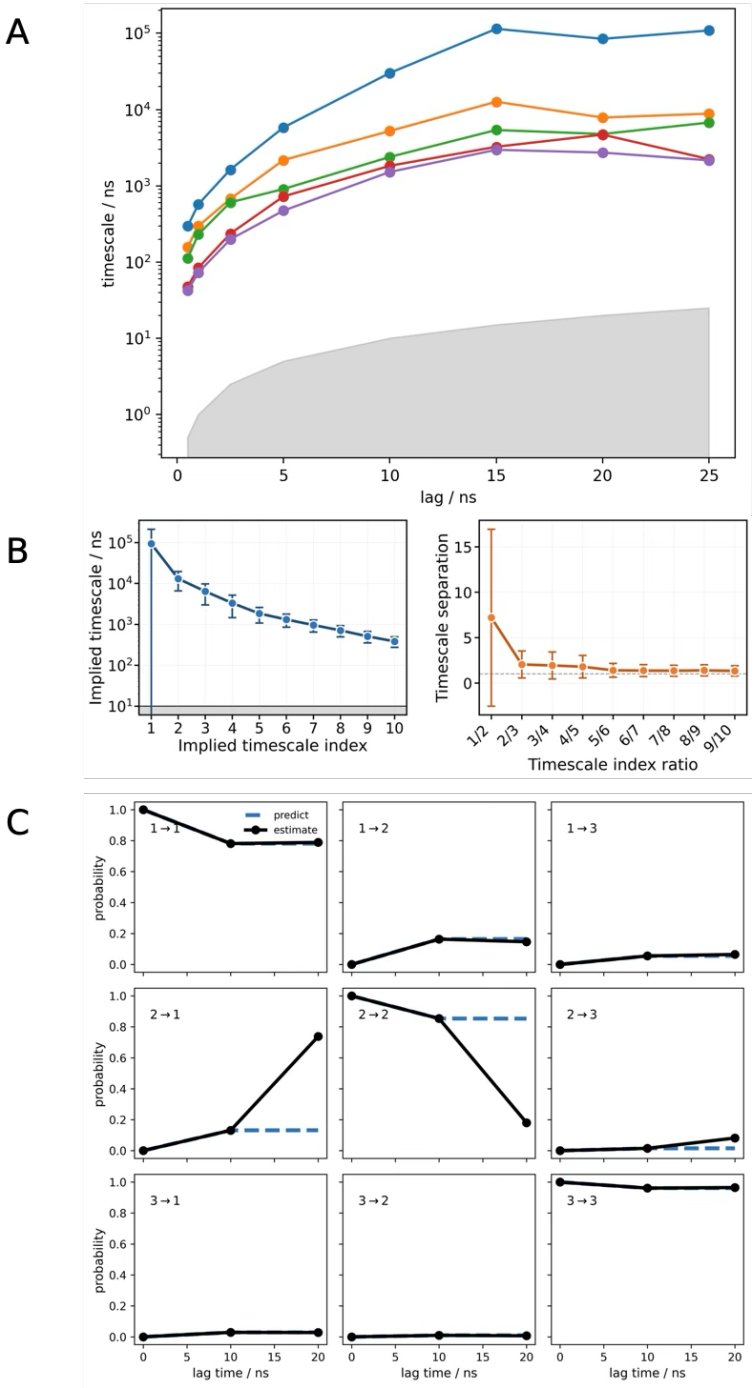

Supplementary Figure 4. The convergence analysis of the simulation with calcium, without PAM_16A (A) Implied timescale (ITS) convergence: the five slowest implied timescales as a function of MSM lag time. Each line is one timescale, ordered from slowest to fastest — timescale 1 (blue), 2 (orange), 3 (green), 4 (red), 5 (purple); the slowest process (blue) is uppermost. The timescales become approximately lag-independent from ~10 ns onward and lie above the grey

region (timescales faster than the lag time, which cannot be resolved). A 10 ns lag time was used for the production MSM.

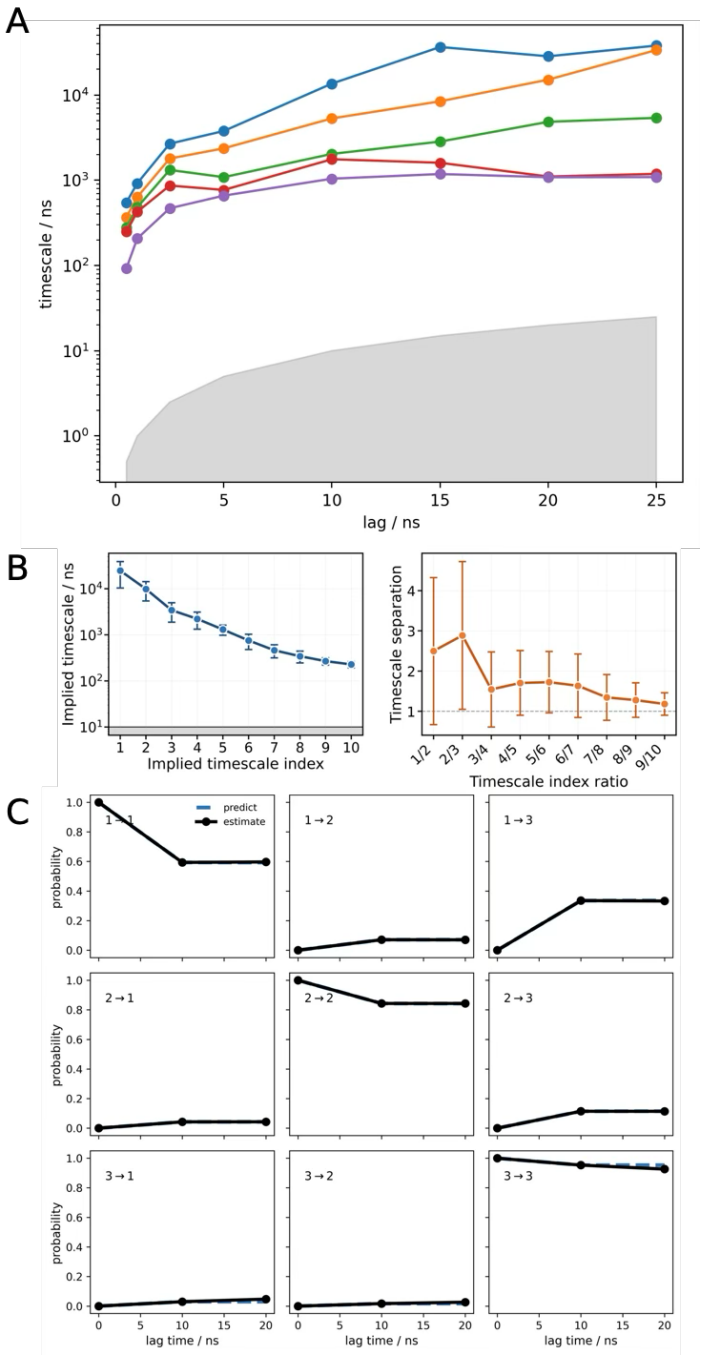

Supplementary Figure 5. The convergence analysis of the simulation with calcium, with PAM_16A (A) Implied timescale (ITS) convergence: the five slowest implied timescales as a function of MSM lag time. Each line is one timescale, ordered from slowest to fastest — timescale 1 (blue), 2 (orange), 3 (green), 4 (red), 5 (purple); the slowest process (blue) is uppermost. The timescales become approximately lag-independent from ~10 ns onward and lie above the grey region (timescales faster than the lag time, which cannot be resolved). A 10 ns lag time was used for the production MSM.

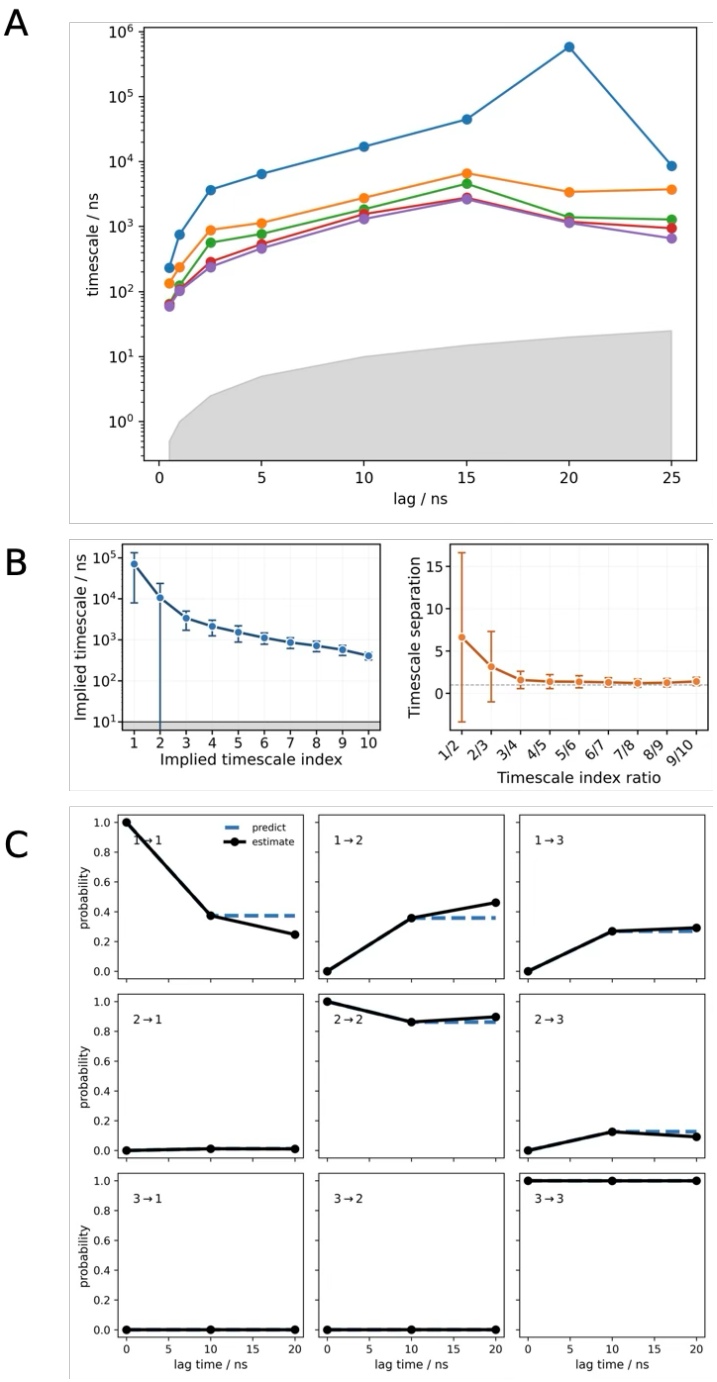

Supplementary Figure 6. The convergence analysis of the simulation without calcium, without PAM_16A (A) Implied timescale (ITS) convergence: the five slowest implied timescales as a function of MSM lag time. Each line is one timescale, ordered from slowest to fastest — timescale 1 (blue), 2 (orange), 3 (green), 4 (red), 5 (purple); the slowest process (blue) is uppermost. The timescales become approximately lag-independent from ~10 ns onward and lie above the grey region (timescales faster than the lag time, which cannot be resolved). A 10 ns lag time was used for the production MSM.

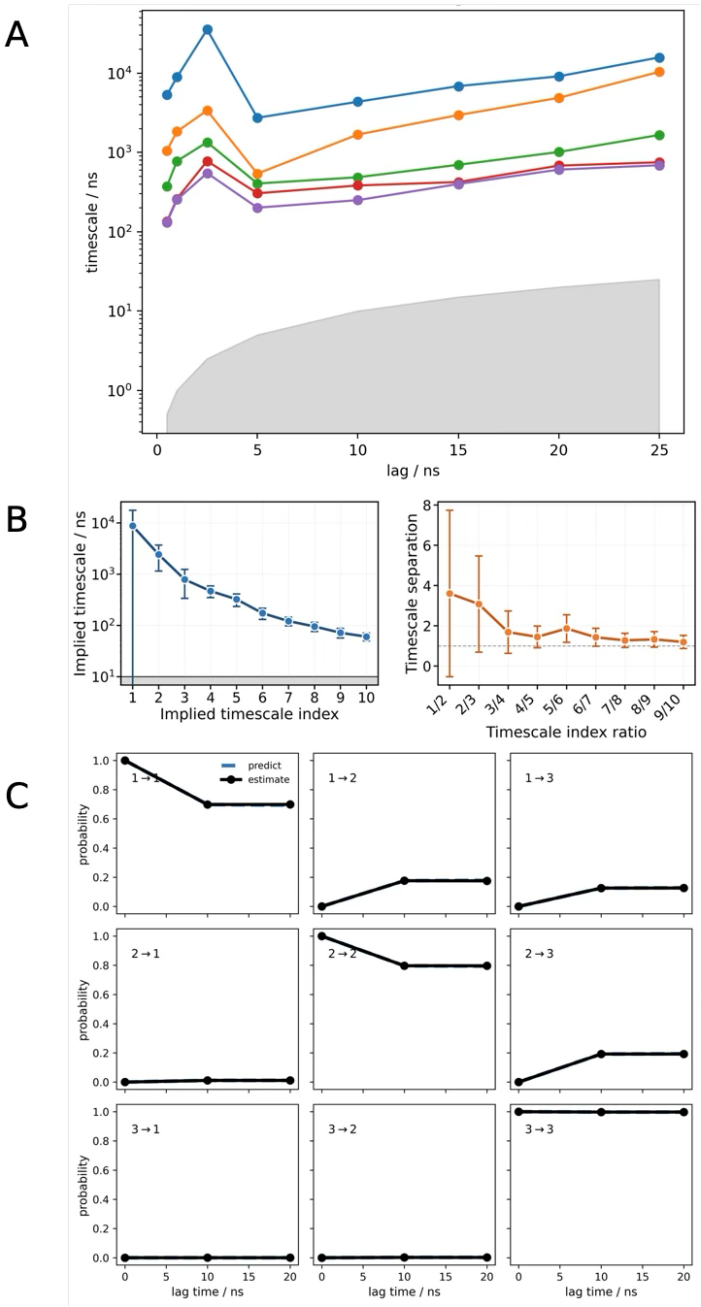

Supplementary Figure 7. The convergence analysis of the simulation without calcium, with PAM_16A (A) Implied timescale (ITS) convergence: the five slowest implied timescales as a function of MSM lag time. Each line is one timescale, ordered from slowest to fastest — timescale 1 (blue), 2 (orange), 3 (green), 4 (red), 5 (purple); the slowest process (blue) is uppermost. The timescales become approximately lag-independent from ~10 ns onward and lie above the grey region (timescales faster than the lag time, which cannot be resolved). A 10 ns lag time was used for the production MSM.

SI Tables

Rank	Predicted site	Aggregate score	ipTM	pTM
1	Calcium-binding site (TM6)	0.294	0.167	0.800
2	Steric gate (TM4–TM6)	0.293	0.166	0.804

Supplementary Table 1. Chai-1 predicted binding poses for PAM_16A on a TMEM16A monomer. The top-ranked clusters fall into two intracellular regions — the steric gate (between TM4 and TM6) and the calcium-binding site (on TM6). The confidence scores for the two sites are comparable.

```
[moleculetype]
; molname       nrexcl
  PAM           2

[atoms]
; id      type   resnr residue atom    cgnr    charge  mass ;  smiles    ; atom_num
   1       TP2d    1   PAM     P01       1       0    36   ;   CO       ; atoms: O2, C18,
   2       SP3d    1   PAM     P02       2       0    54   ;   NC=O     ; atoms: O3, N5, C16,
   3       TN5a    1   PAM     N01       3       0    36   ;   CN       ; atoms: N6, C22,
   4       SC3     1   PAM     C01       4       0    54   ;   CCC      ; atoms: C7, C8, C9,
   5       SP3d    1   PAM     P03       5       0    54   ;   NC=O     ; atoms: O1, N4, C11,
   6       TC4     1   PAM     C02       6       0    36   ;   CC       ; atoms: C10, C12,
   7       TC5     1   PAM     C03       7       0    36   ;   C=C      ; atoms: C13, C15,
   8       TC5     1   PAM     C04       8       0    36   ;   C=C      ; atoms: C14, C20,
   9       TC5     1   PAM     C05       9       0    36   ;   C=C      ; atoms: C21, C24,
   10      SX3     1   PAM     X01       10      0    54   ;   C=CCl    ; atoms: Cl0, C19, C23,
   11      TC6     1   PAM     C06       11      0    36   ;   C#C      ; atoms: C17, C25,


[bonds]
;  i   j     funct   length   force.c.
   1   6      1       0.29      25000.00
   1   9      1       0.28      25000.00
   2   6      1       0.22      100000.00
   2   8      1       0.23      100000.00
   3   7      1       0.30      25000.00
   3   8      1       0.22      25000.00
   4   5      1       0.27      25000.00
   4   11     1       0.33      10000.00
   5   7      1       0.26      25000.00
   6   10     1       0.33      10000.00
   7   8      1       0.27      25000.00
   9   10     1       0.30      5000.00
[constraints]
;  i   j     funct   length
   6   9      1       0.43
   1   10     1       0.42

[angles]
;  i  j  k    funct  angle  force.c.
   1  2  6       1    58.9    30.0
   1  2  8       1    132.6   30.0
   1  3  7       1    30.9   100.0
   1  3  8       1    31.8   100.0
   1  4  5       1    23.8   100.0
   1  4 11       1    82.3    30.0
   1  5  7       1    20.2    30.0
   1  6  3       1    83.8   100.0
   1  6  4       1    57.1   250.0
   1  6  5       1    59.7   250.0
   1  6  7       1    59.4   100.0
   1  6  8       1    87.4   100.0
   1  6  9       1    39.8   100.0
   1  6 10       1    83.6   250.0
   1  6 11       1    60.0   100.0
   1  7  8       1    85.7   100.0
   1  9  2       1    36.2   250.0
   1  9  3       1    44.0   100.0
   1  9  4       1    46.7   250.0
   1  9  5       1    39.1   250.0
   1  9  7       1    32.1   100.0
```

```
1  9  8      1    41.4   100.0
1  9 10      1    92.6   250.0
1  9 11      1    31.4   100.0
1 10  2      1    44.5   100.0
1 10  3      1    54.1    30.0
1 10  4      1    38.3   100.0
1 10  5      1    36.4   100.0
1 10  7      1    34.1    30.0
1 10  8      1    52.9    30.0
1 10 11      1    28.4    30.0
2  3  7      1    51.9   100.0
2  4  5      1    9.3     25.0
2  8  4      1    124.5  100.0
2  8  5      1    116.9  100.0
2  8 11      1    115.2  100.0
3  4  5      1    28.6   100.0
3  7  4      1    81.5   250.0
3  7 11      1    92.9   100.0
4  5 11      1    60.4    45.0
```

Supplementary Table 2. MARTINI-3 coarse-grained topology of PAM_16A generated with AutoMartini3. Bead types and atom-to-bead assignments ([atoms]), together with the bonded parameters ([bonds], [constraints], [angles]) used in the coarse-grained flooding simulations.